2018 IEEE Intelligent Vehicles Symposium (IV)
Changshu, Suzhou, China, June 26-30, 2018

Near-Optimal Online Motion Planning of Connected and Automated Vehicles at a Signal-Free and Lane-Free Intersection *

Bai Li, Youmin Zhang, Yue Zhang, Ning Jia, and Yuming Ge

***Abstract*—In this paper, we propose a cooperative motion planning method for a group of connected and automated vehicles (CAVs) crossing a lane-free intersection without using explicit traffic signaling. This multi-vehicle motion planning task is formulated as a centralized optimal control problem. However, the solution to this optimal control problem is numerically intractable due to the high dimensionality of the collision-avoidance constraints and the nonlinearity of the vehicle kinematics. A two-stage strategy is proposed for generating online solutions: at Stage 1, the CAVs are requested to reach a standard formation before entering the intersection; at Stage 2, the vehicles cross the intersection. As the motion planning sub-problem at Stage 2 begins with a standard configuration, the optimal solution to this standard sub-problem can be computed offline in advance and applied online directly. On the other hand, the formation reconfiguration sub-problem at Stage 1 is easy to solve online. Through dividing the entire dynamic process into two periods, the difficulties in the original optimal control problem are significantly reduced so that the real-time performance is achieved.**

I. Introduction

Autonomous intersection management (AIM) plays a key role in the development of intelligent transportation systems, and is going through revolutionary changes brought by the connected and automated vehicles (CAVs) [1]. However, the benefit of using CAVs to improve the intersection throughput is not maximized because the cooperative capability among vehicles has not been seriously considered [2]. Concretely, the CAVs' pass-through paths are fixed or restricted to a small number of types in most of the existing AIM methods [3–8], which indicates the CAVs' mobility is far from being fully exploited.

The goal of this work is to propose a lane-free AIM method which can activate the cooperation potential in a multi-CAV team. To this end, the AIM scheme is described as a multi-vehicle motion planning (MVMP) problem, wherein each vehicle can drive with more flexibilities in the intersection scenario without the concept of lanes at all. We use a computational optimal control approach, together with a stage division strategy, to solve this MVMP problem online.

The rest of this paper is organized as follows. Section II introduces the MVMP problem formulation. Section III briefly introduces the way to obtain offline optimal solutions to the MVMP problems. Section IV introduces a two-stage online motion planning method. Simulation and discusses are provided in Section V. Section VI concludes the paper.

II. MVMP Problem Formulation

The AIM oriented MVMP problem is formulated as a centralized optimal control problem so as to minimize delays in the intersection, subject to vehicle dynamics, safety constraints and space limitations. All the vehicles are assumed to be CAVs in the current work.

A. Vehicle Kinematic Constraints

Suppose N_V CAVs aim to cross the intersection. CAV i ($i = 1,...,N_V$) is governed by the kinematic bicycle model [2], that is,

$$\frac{\mathrm{d}}{\mathrm{d}t}\begin{bmatrix} x_i(t) \\ y_i(t) \\ \theta_i(t) \\ v_i(t) \\ \phi_i(t) \end{bmatrix} = \begin{bmatrix} v_i(t)\cdot\cos\theta_i(t) \\ v_i(t)\cdot\sin\theta_i(t) \\ v_i(t)\cdot\tan\phi_i(t)/\mathrm{L_w} \\ a_i(t) \\ \omega_i(t) \end{bmatrix},\ t\in[t_0,t_\mathrm{f}], \tag{1}$$

where t_0 and t_f respectively denotes the starting and terminal time for crossing the intersection, $(x_i(t), y_i(t))$ represents the midpoint along the rear-wheel axis, $v_i(t)$ and $a_i(t)$ denote the velocity and acceleration of that point, respectively, $\phi_i(t)$ represents the steering angle, $\omega_i(t)$ refers to the angular velocity of $\phi_i(t)$, $\theta_i(t)$ represents the orientation angle of the vehicle, and $\mathrm{L_w}$ denotes the distance between the front and rear wheel axes (Fig. 1).

To ensure that the state/control variables are within rational ranges, the following constraints are imposed:

$$|a_i(t)| \le \mathrm{a_{max}}, \tag{2a}$$

$$0 \le v_i(t) \le \mathrm{v_{max}}, \tag{2b}$$

* This work was supported by the National Natural Science Foundation of China under Grant 61573282 and 71571132, Shaanxi Province Natural Science Foundation under Grant 2015JZ020, and the Natural Sciences and Engineering Research Council of Canada.

Bai Li is with the Shaanxi Key Laboratory of Complex System Control and Intelligent Information Processing, Xi'an University of Technology, Xi'an 710048, China, and the College of Control Science and Engineering, Zhejiang University, Hangzhou 310027, China (e-mail: libai@zju.edu.cn).

Youmin Zhang is with the Department of Mechanical, Industrial and Aerospace Engineering, Concordia Institute of Aerospace Design and Innovation, Concordia University, Montreal, Canada (phone: 514-848-2424 ext. 5225; fax: 514-848-3175; e-mail: ymzhang@encs.concordia.ca).

Yue Zhang is with the Division of Systems Engineering, and Center for Information and Systems Engineering, Boston University, Boston, MA 02215, USA (e-mail: joycez@bu.edu).

Ning Jia is with the Institute of Systems Engineering, Tianjin University, Tianjin 300072, China (e-mail: jia_ning@tju.edu.cn).

Yuming Ge is with the China Academy of Information and Communications Technology, Beijing 100191, China (e-mail: geyuming @caict.ac.cn).

$$|\phi_i(t)| \le \Phi_{\max}, \tag{2c}$$

$$|\omega_i(t)| \le \Omega_{\max},\ t \in [t_0, t_f], \tag{2d}$$

where $a_{\max}$, $v_{\max}$, $\Phi_{\max}$, and $\Omega_{\max}$ denote the upper bounds for $|a_i(t)|$, $v_i(t)$, $|\phi_i(t)|$, and $|\omega_i(t)|$, respectively.

B. Collision Avoidance Constraints

In addition to the vehicle kinematics, collision avoidance constraints within the intersection are also imposed. Suppose that each CAV is rectangular. This work uses a circumcircles to represent each vehicle. As depicted in Fig. 1, the circle center (x_{Ci}, y_{Ci}) locates at the geometric center of vehicle i, and the radius R_i can be uniformly determined as follows:

$$\begin{aligned} x_{Ci}(t) &= x_i(t) + \left(\frac{L_w + L_f - L_r}{2}\right)\cdot\cos(\theta_i(t)), \\ y_{Ci}(t) &= y_i(t) + \left(\frac{L_w + L_f - L_r}{2}\right)\cdot\sin(\theta_i(t)), \\ R_i &= \frac{1}{2}\sqrt{(L_r + L_w + L_f)^2 + (L_b)^2}. \end{aligned} \tag{3}$$

This representation practically useful in the sense that the redundant half-moon regions are regarded as safety oriented margins. Under such simplification, collisions among the vehicles can be avoided if the following constraint is satisfied throughout the trajectory,

$$\begin{aligned} &\left(x_{Ci}(t) - x_{Cj}(t)\right)^2 + \left(y_{Ci}(t) - y_{Cj}(t)\right)^2 \ge (R_i + R_j)^2, \\ &\forall i, j = 1, \ldots, N_V,\ i \ne j,\ t \in [t_0, t_f]. \end{aligned} \tag{4}$$

In addition to vehicle-to-vehicle collision avoidance, the CAVs should not collide with the street blocks as well. As shown in Fig. 2, the circle represents the vehicle, while the rectangle MNPQ represents one street block. To make sure that the circle is not overlapped with the rectangle MNPQ, the circle center (x_{Ci}, y_{Ci}) should remain out of a specified roundrect region surrounds rectangle MNPQ (Fig. 2). Since a roundrect region is not easy to describe, it is slightly slacked as a standard rectangle M'N'P'Q' (see Fig. 2). Regarding how to restrict the circle center (x_{Ci}, y_{Ci}) from entering rectangular region M'N'P'Q', an analytical criterion called Triangle Area Criterion is adopted. Details can be found in [9].

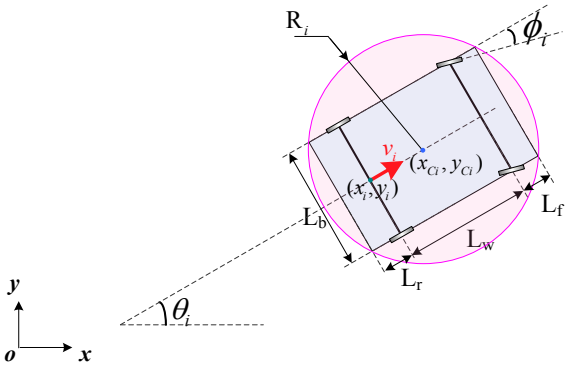

Fig. 1. Schematics on the kinematic model of a front steering CAV. L_b, L_r, L_w, and L_f determine the geometric shape.

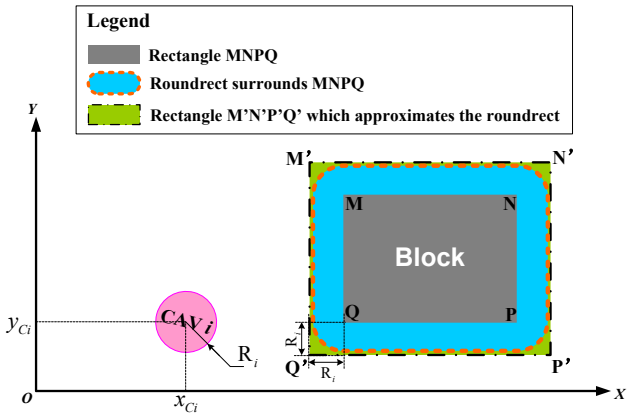

Fig. 2. Schematics on the formulation of collision avoidance condition between a circle and a rectangle.

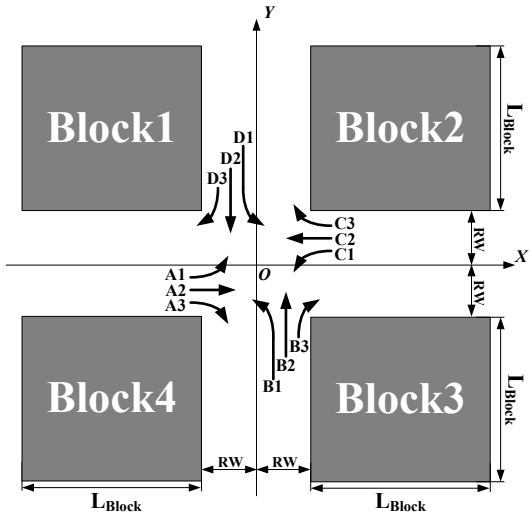

Fig. 3. Schematics on the intersection scenario and CAV categories.

A 2-D coordinate system is set up to represent the intersection, while the x and y axes represent the central lines of the intersection (Fig. 3). The length of each street block is denoted as L_{Block}, which is assumed to be sufficiently large. The road width is set to $2 \cdot RW$. Each CAV should not collide with the street block barriers defined in this x-y coordinate. The detailed constraints are omitted here.

C. Space Constraints

Each CAV is allowed to run only in specified regions of the whole intersection space.

Assume that each CAV will enter the intersection from one of the four directions and exit in one of the following three ways: left turn, going straight, right turn. Hence, all the intersection-crossing CAVs are classified into 12 categories depending on the direction from which the vehicle enters and the direction towards which the vehicle exits. In Fig. 3, A1, B1, C1, and D1 represent the vehicles which come from four different directions and aim to make left turns; A2, B2, C2, and D2 represent the vehicles which aim to go straight; A3, B3, C3, and D3 represent the vehicles which intend to make right turns.

The allowable region for each CAV category may be

bounded by x and y axes and the street block curbs. An example is highlighted in Fig. 4(a) showing the allowable region for vehicles coming from west and turning right, i.e., A3 category. For vehicles going straight, i.e., A2 category, the allowable region is bounded by x axis and the street block curb $y=-\mathrm{RW}$. For the A1 vehicles, the allowable region completely covers the allowable region for D3 category, which enables the left-turn vehicles to drive with more flexibility (see the left-turn path in Fig. 4(a) as an example). Counterintuitively from the conventional traffic viewpoint, this flexibility offers benefit under the scenario with heavy left-turn traffic flow [10]. The allowable regions for the CAVs in the rest 9 categories can be defined in the same way.

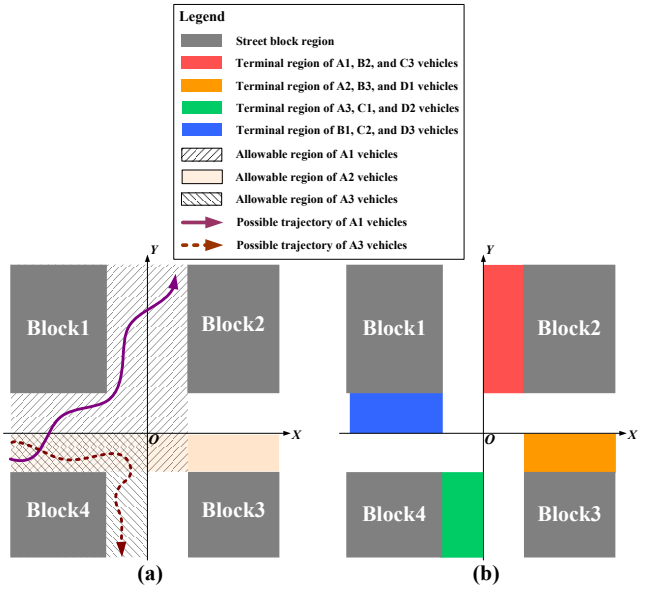

Fig. 4. Schematics on the space constraints: (a) allowable regions of A1, A2, and A3 vehicles; (b) terminal regions of different CAVs.

D. Initial and Terminal Conditions

Since $t=t_0$, all the CAVs are taken over by the AIM system. For vehicle i, $[x_i(t_0), y_i(t_0)]$ is given by the sensors, the orientation variable $\theta_i(t_0)$ should ensure the vehicle is driving along the current lane, and the other initial state/control variables are assumed to be

$$[v_i(t_0), a_i(t_0), \phi_i(t_0), \omega_i(t_0)] = [\mathrm{v}_0, 0, 0, 0],\ i=1,2,...,\mathrm{N_V}, \quad (5)$$

where v_0 is a constant of velocity. Eq. (5) ensures a feasible initial state in the sense that, even if the gap between two adjacent vehicles is quite small, the same speed and same control input at $t=t_0$ can still guarantee that no collision would occur after t_0 between the two vehicles. Due to the same concern, the terminal condition of each CAV is set to

$$[v_i(t_\mathrm{f}), a_i(t_\mathrm{f}), \phi_i(t_\mathrm{f}), \omega_i(t_\mathrm{f})] = [\mathrm{v}_0, 0, 0, 0],\ i=1,2,...,\mathrm{N_V}. \quad (6)$$

Each vehicle should reach a specific state at the terminal instant t_f. Let us take the CAVs in A1 category for example. At $t=t_\mathrm{f}$, the vehicles should reach the target road region (for A1 vehicle, see the red region highlighted in Fig. 4(b)). Also, the driving orientations of the vehicles should be parallel to their target roads at the terminal moment. These terminal conditions can be summarized as

$$\begin{cases} y_{Ci}(t_\mathrm{f}) - \mathrm{R}_i \ge 0 \\ x_{Ci}(t_\mathrm{f}) - \mathrm{R}_i \ge \mathrm{RW},\ i \in \mathrm{A1} \cup \mathrm{B2} \cup \mathrm{C3}; \\ \theta_i(t_\mathrm{f}) = \pi/2 \end{cases}$$
$$\begin{cases} y_{Ci}(t_\mathrm{f}) - \mathrm{R}_i \ge 0 \\ x_{Ci}(t_\mathrm{f}) + \mathrm{R}_i \le -\mathrm{RW},\ i \in \mathrm{B1} \cup \mathrm{C2} \cup \mathrm{D3}; \\ \theta_i(t_\mathrm{f}) = \pi \end{cases}$$
$$\begin{cases} y_{Ci}(t_\mathrm{f}) + \mathrm{R}_i \le 0 \\ x_{Ci}(t_\mathrm{f}) + \mathrm{R}_i \le -\mathrm{RW},\ i \in \mathrm{A3} \cup \mathrm{C1} \cup \mathrm{D2}; \\ \theta_i(t_\mathrm{f}) = -\pi/2 \end{cases} \quad (7)$$
$$\begin{cases} y_{Ci}(t_\mathrm{f}) + \mathrm{R}_i \le 0 \\ x_{Ci}(t_\mathrm{f}) - \mathrm{R}_i \ge \mathrm{RW},\ i \in \mathrm{A2} \cup \mathrm{B3} \cup \mathrm{D1}. \\ \theta_i(t_\mathrm{f}) = 0 \end{cases}$$

E. Optimization Objective

The problem is formulated so as to jointly penalize large completion time, and encourage the CAVs to go farther in their terminal regions:

$$\text{minimize}: \quad (t_\mathrm{f} - t_0) - \lambda \cdot \Bigg(\sum_{i \in \mathrm{A1} \cup \mathrm{B2} \cup \mathrm{C3}} y_i(t_\mathrm{f}) + \sum_{i \in \mathrm{A2} \cup \mathrm{B3} \cup \mathrm{D1}} x_i(t_\mathrm{f}) - \sum_{i \in \mathrm{A3} \cup \mathrm{C1} \cup \mathrm{D2}} y_i(t_\mathrm{f}) - \sum_{i \in \mathrm{B1} \cup \mathrm{C2} \cup \mathrm{D3}} x_i(t_\mathrm{f}) \Bigg). \quad (8)$$

Expecting the vehicles to go farther and to complete the process in less time are conflicting. The rationale of designing such an optimization objective is given as follows [11]. As there are multiple vehicles in the scenario, $(t_\mathrm{f} - t_0)$ is directly determined by the last CAV that can satisfy the terminal condition. The rest vehicles which can reach their terminal regions earlier would not be clearly directed without the second item in (8). Therefore, although conflicts exist in (8), that would not be a problem if the weight parameter $\lambda > 0$ is set sufficiently small.

F. Overall Optimal Control Problem Formulation

The optimal control problem is summarized as

$$\begin{aligned} &\text{minimize} \quad (8) \\ &\text{s.t. vehicle kinematic constraints (1) and (2);} \\ &\quad \text{vehicle-to-vehicle collision-free constraints (3), (4);} \\ &\quad \text{vehicle-to-block collision-free constraints;} \\ &\quad \text{allowable space constraints;} \\ &\quad \text{initial and terminal conditions (5)} - \text{(7)}. \end{aligned} \quad (9)$$

The decision variables include $a_i(t)$, $\omega_i(t)$ ($i=1,...,\mathrm{N_V}$), and t_f.

III. Offline Motion Planning Method

To solve (9) numerically, the orthogonal collocation direct transcription (OCDT) method is adopted, which approximates each continuous variable in (9) via a finite number of parameters [12], thereby converting (9) to a nonlinear programming (NLP) problem. The main difficulties in solving (9), when it is discretized to an NLP problem, lie in the high-dimensional collision avoidance constraints among the CAVs and the nonlinear kinematics-related equations.

The interior-point method (IPM) is an efficient solver for large-scale NLP problems [13]. However, simply adopting IPM cannot solve the complicated NLP problem concerned in this work. To facilitate the solving process, a progressively constrained dynamic optimization (PCDO) method [2] is utilized. Through using OCDT+IPM+PCDO, the offline numerical solutions to (9) are obtained. The offline computation procedure serves as a preliminary step for deriving online solutions.

IV. Online Motion Planning Method

A. Motivation

To find online NLP solutions, one should not expect the existing offline computation methods to execute in real time, or to expect significant progress in processor manufacture. Instead, a promising way is to avoid the complicated online computation. To this end, a natural idea is to solve the NLP problems offline and store the solutions for online usage. As the number of cases is infinite, it is necessary to select a finite number of "typical" cases, and then to solve them offline in advance. Following this idea, two issues should be addressed: 1) how to select the typical offline cases, and 2) how to utilize the offline solution to a typical case in solving a new case online.

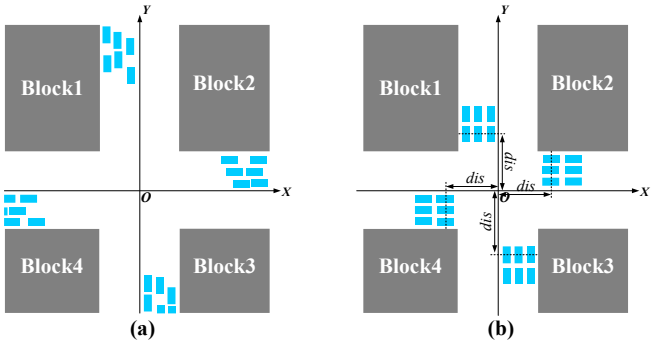

Fig. 5. Schematics on the CAV platoon formation: (a) a generic case; (b) a typical case in association with (a).

According to the formulation (9), the differences among the cases are determined by the initial location (i.e. $[x_i(t_0), y_i(t_0)]$) and the intersection exit direction of each CAV. Suppose a generic case depicted in Fig. 5(a) is assigned online. We request the CAVs to reach a specified formation shown in Fig. 5(b) before crossing the intersection. This means the entire intersection-crossing process should be divided into two stages: at Stage 1, the CAVs reconfigure the formation from Fig. 5(a) to Fig. 5(b); at Stage 2, the CAVs cross the intersection. The formation reconfiguration process at Stage 1 is easy, thus the MVMP sub-problem can be solved fast. Since Stage 2 begins with a specified configuration, thus it is not relevant to Stage 1, which indicates that the MVMP sub-problem at Stage 2 can be prepared offline in advance and used online directly. In this way, the difficulties in the original problem (9) are avoided in finding the online solution. The details are given in the next subsection.

B. Two-Stage Online Motion Planning Method

Let us define a number of typical cases, wherein the initial multi-CAV formation is "tidy". Herein, the tidiness is reflected in two aspects: 1) along each leg of the 4-leg intersection, the CAVs are running in equidistant rows and columns with the same acceleration, velocity, orientation; 2) the distance between the first-row vehicles in each leg and the intersection center is identical. Since each CAV has 3 possible exit ways, the aforementioned tidy formation represents 3^{N_V} different cases. We regard this tidy formation as the "standard formation", and regard those 3^{N_V} specific cases as "standard cases" in the rest of this paper. As the exit intention of each CAV is not known *a priori*, all of the standard cases should be solved offline for preparation.

To transform a generic problem to one of the standard problems, a formation reconfiguration stage is needed. The corresponding MVMP sub-problem is easy, because the CAVs in different legs of the intersection are independent, that is, they have no chance to collide. Furthermore, we request that the CAVs should not change lanes at Stage 1, i.e.,

$$[\theta_i(t), a_i(t), \omega_i(t)] \equiv [\theta_i(t_0), 0, 0],\ t \in [t_0, t_1], \tag{10}$$

wherein $[t_0, t_1]$ denotes the duration of Stage 1. Under such condition, the complicated kinematic system (1) degrades to be linear:

$$\frac{\mathrm{d}}{\mathrm{d}t}\begin{bmatrix} x_i(t) \\ y_i(t) \\ v_i(t) \end{bmatrix} = \begin{bmatrix} v_i(t)\cdot\cos\theta_i(t_0) \\ v_i(t)\cdot\sin\theta_i(t_0) \\ a_i(t) \end{bmatrix},\ t \in [t_0, t_1]. \tag{11}$$

Also, the quadratic collision-avoidance constraints (4) are simplified as linear inequalities in smaller scales because each CAV only has chances to collide with its adjacent neighbors in the same lane. The following constraints ensure that CAV i does not collide with its adjacent neighbors m and n in the same lane if i, m, n are from $\mathrm{A1}\bigcup\mathrm{A2}\bigcup\mathrm{A3}$ for example:

$$\begin{aligned} x_{Ci}(t) - x_{Cm}(t) &\geq \mathrm{R}_i + \mathrm{R}_m \\ x_{Cn}(t) - x_{Ci}(t) &\geq \mathrm{R}_i + \mathrm{R}_n \end{aligned},\ t \in [t_0, t_1]. \tag{12}$$

Eq. (10) also ensures that each CAV has no chance to collide with the street block barriers.

At the terminal moment of Stage 1, the CAVs should form a standard formation depicted in Fig. 5(b). This means the location of each CAV is specified:

$$[x_{Ci}(t_1), y_{Ci}(t_1)] = [\hat{\mathrm{x}}_i, \hat{\mathrm{y}}_i],\ i = 1, 2, ..., \mathrm{N_V}, \tag{13}$$

wherein each $[\hat{\mathrm{x}}_i, \hat{\mathrm{y}}_i]$ is given. Similar with (6), the CAVs

should run with in safe state at t_1, i.e.,

$$[v_i(t_1), a_i(t_1)] = [v_0, 0],\ i = 1, 2, ..., N_V. \quad (14)$$

As a summary, the formation reconfiguration MVMP sub-problem is formulated as

$$\begin{aligned} &\text{minimize } (t_1 - t_0) \\ &\text{s.t. vehicle kinematic constraints (10), (11);} \\ &\quad \text{vehicle-to-vehicle collision-free constraints like (12);} \\ &\quad \text{initial and terminal conditions (5), (13), (14).} \end{aligned} \quad (15)$$

Compared with (9), (15) does not contain complicated kinematics or large-scale collision-avoidance constraints, thus is easier to solve. The solution to (15), when derived online, is implemented at Stage 1. At the end of Stage 1, the formation of the CAV platoon becomes standard. Thereafter, Stage 2 begins, during which the offline solution to the standard problem is extracted and implemented.

The pseudo-code of the two-stage online MVMP method is summarized in Algorithm 1.

Algorithm 1. Online MVMP Algorithm.

1. Load the assigned online MVMP problem;
2. Solve (15) using OCDT+IPM, record the solution in χ_1;
3. Extract the corresponding offline standard solution, record it in χ_2;
4. Combine χ_1 with χ_2, output the result;
5. Exit.

Note that steps 2 and 3 are independent, thus executing them in parallel, if possible, would further reduce the online computational time.

V. Numerical Experiments and Discussions

Simulations were carried out in the AMPL environment [14] and executed on an Intel Core i5-4460T CPU that runs at 1.90 GHz. IPOPT (version 3.12.1, a software package of IPM) is utilized [13]. Some critical parametric settings are listed in Table I. A video with detailed simulation results is provided to assist understanding at https://youtu.be/88n3iJhpQCM.

Table I. Parametric notations and settings.

Parameter	Description	Setting
N_{fe}	Number of finite elements in OCDT	10
N_V	Number of CAVs	24
L_f	Vehicle front overhang length	0 m
L_w	Vehicle wheelbase	2.545 m
L_r	Vehicle rear overhang length	0 m
L_b	Vehicle width	2.545 m
RW	Road width	11.25 m
λ	Trade-off parameter in (8)	10^{-5}
v_{max}	Upper bound of $v_i(t)$, $i = 1, 2, ...N_v$	15.0 m/s
Φ_{max}	Upper bound of $\lvert\phi_i(t)\rvert$, $i = 1, 2, ...N_v$	0.576 rad
a_{max}	Upper bound of $\lvert a_i(t)\rvert$, $i = 1, 2, ...N_v$	0.5 m/s^2
ω_{max}	Upper bound of $\lvert\omega_i(t)\rvert$, $i = 1, 2, ...N_v$	0.5 rad/s
v_0	Common velocity at stage boundaries	10.0 m/s

A. On the Performance of Offline Solutions

Fig. 6 illustrates the offline solution to one standard case, wherein the exit intention of each CAV is randomly assigned (details of the experiment setup of this case are listed in Appendix). In Fig. 6, the usage of opposite side of the road can be observed for some of the CAVs. Also, the CAVs are able to travel flexibly without the need to keep in one lane during the entire dynamic process, which contributes to a full usage of the road space.

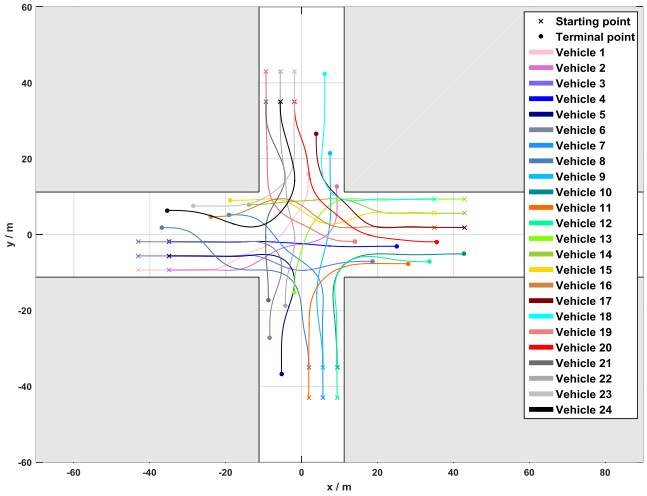

Fig. 6. Simulation results of an offline case.

Computation of this case took less than 300 seconds. Suppose each standard case takes 400 seconds to solve offline on average, then all the offline cases would take 564,859,072,962 seconds to finish. If 10,000 computers work simultaneously, 358.22 years would be needed to build a complete standard case set. This indicates the proposed method still deserves improvement.

B. On the Performance of Online Solutions

This subsection is about the computational efficiency of the two-stage online MVMP strategy. Since Stage 2 does not need any online computation resource, let us focus on the computational speed of the formation reconfiguration MVMP sub-problem at Stage 1. Repeated experiments with randomly generated initial formations were conducted. The initial distance between each vehicle and the intersection center is set as a stochastic value that uniformly ranges between 100 m and 110 m. As it turned out, the average computation time of 3,000 repeated experiments is 0.4015 sec (best 0.3830 sec, worst 0.5172 sec, median 0.4036 sec, and standard deviation 0.0109). This indicates that the MVMP sub-problem at Stage 1 is stable thus being suitable for online computation.

VI. Conclusions

This paper has presented an AIM oriented online MVMP method for a number of CAVs crossing a signal-free and lane-free intersection. The main contributions lie in 1) the accurate and unified formulation of the problem as an optimal control problem; 2) the way to generate online solutions.

As the future work, a few slight changes will be made so that this two-stage method would be able to handle

continuous traffic flows.

ACKNOWLEDGMENTS

The authors are sincerely grateful to the two anonymous reviewers for their valuable comments. Bai Li thanks Dr. Zhijiang Shao for the inspirations and suggestions.

APPENDIX

The initial location and driving intention of each CAV is listed in the following table.

Table A. Experiment setup of the initial configurations.

CAV #	Initial location	Category
1	$[\hat{x}_1, \hat{y}_1] = [-43, -9.375]$	A1
2	$[\hat{x}_2, \hat{y}_2] = [-35, -9.375]$	A1
3	$[\hat{x}_3, \hat{y}_3] = [-43, -5.625]$	A2
4	$[\hat{x}_4, \hat{y}_4] = [-35, -1.875]$	A2
5	$[\hat{x}_5, \hat{y}_5] = [-35, -5.625]$	A3
6	$[\hat{x}_6, \hat{y}_6] = [-43, -1.875]$	A3
7	$[\hat{x}_7, \hat{y}_7] = [5.625, -43]$	B1
8	$[\hat{x}_8, \hat{y}_8] = [1.875, -43]$	B1
9	$[\hat{x}_9, \hat{y}_9] = [5.625, -35]$	B2
10	$[\hat{x}_{10}, \hat{y}_{10}] = [9.375, -35]$	B3
11	$[\hat{x}_{11}, \hat{y}_{11}] = [1.875, -43]$	B3
12	$[\hat{x}_{12}, \hat{y}_{12}] = [9.375, -43]$	B3
13	$[\hat{x}_{13}, \hat{y}_{13}] = [43, 9.375]$	C1
14	$[\hat{x}_{14}, \hat{y}_{14}] = [43, 5.625]$	C2
15	$[\hat{x}_{15}, \hat{y}_{15}] = [35, 5.625]$	C2
16	$[\hat{x}_{16}, \hat{y}_{16}] = [35, 1.875]$	C2
17	$[\hat{x}_{17}, \hat{y}_{17}] = [43, 1.875]$	C3
18	$[\hat{x}_{18}, \hat{y}_{18}] = [35, 9.375]$	C3
19	$[\hat{x}_{19}, \hat{y}_{19}] = [-9.375, 43]$	D1
20	$[\hat{x}_{20}, \hat{y}_{20}] = [-1.875, 35]$	D1
21	$[\hat{x}_{21}, \hat{y}_{21}] = [-9.375, 35]$	D2
22	$[\hat{x}_{22}, \hat{y}_{22}] = [-5.625, 43]$	D2
23	$[\hat{x}_{23}, \hat{y}_{23}] = [-1.875, 43]$	D3
24	$[\hat{x}_{24}, \hat{y}_{24}] = [-5.625, 35]$	D3

REFERENCES

[1] L. Chen, and C. Englund, "Cooperative intersection management: A survey," *IEEE Transactions on Intelligent Transportation Systems*, vol. 17, no. 2, pp. 570–586, 2016.

[2] B. Li, Y. M. Zhang, Z. Shao, and N. Jia, "Simultaneous versus joint computing: A case study of multi-vehicle parking motion planning," *Journal of Computational Science*, vol. 20, pp. 30–40, 2017.

[3] Y. Zhang, A. A. Malikopoulos, and C. G. Cassandras, "Optimal control and coordination of connected and automated vehicles at urban traffic intersections," In *Proc. 2016 IEEE American Control Conference,* pp. 6227–6232, 2016.

[4] M. W. Levin, and D. Rey, "Conflict-point formulation of intersection control for autonomous vehicles," *Transportation Research Part C: Emerging Technologies*, vol. 85, pp. 528–547, 2017.

[5] K. Dresner, and P. Stone, "A multi-agent approach to autonomous intersection management," *Journal of Artificial Intelligence Research*, vol. 31, pp. 591–656, 2008.

[6] I. H. Zohdy, R. K. Kamalanathsharma, and H. Rakha, "Intersection management for autonomous vehicles using iCACC," In *Proc. IEEE International Conference on Intelligent Transportation Systems*, pp. 1109–1114, 2012.

[7] A. Lombard, F. Perronnet, A. Abbas-Turki, and A. E. Moudni, "Decentralized management of intersections of automated guided vehicles," *IFAC-PapersOnLine*, vol. 49, no. 12, pp. 497–502, 2016.

[8] J. Gregoire, S. Bonnabel, and A. L. Fortelle, "Optimal cooperative motion planning for vehicles at intersections," HAL-INRIA, 2012.

[9] B. Li, and Z. Shao, "A unified motion planning method for parking an autonomous vehicle in the presence of irregularly placed obstacles," *Knowledge-Based Systems*, vol. 86, pp. 11–20, 2015.

[10] R. Goldblatt, F. Mier, and J. Friedman, "Continuous flow intersections," *Institute of Transportation Engineers Journal*, vol. 64, pp. 35–35, 1994.

[11] B. Li, and Y. M. Zhang, "Fault-tolerant cooperative motion planning of connected and automated vehicles at a signal-free and lane-free intersection," In *Proc. 10th IFAC Symposium on Fault Detection, Supervision and Safety for Technical Processes*, accepted, 2018.

[12] B. Li, H. Liu, D. Xiao, G. Yu, and Y. M. Zhang, "Centralized and optimal motion planning for large-scale AGV systems: A generic approach," *Advances in Engineering Software*, vol. 106, pp. 33–46, 2017.

[13] A. Wächter, and L. Biegler, "On the implementation of an interior-point filter line-search algorithm for large-scale nonlinear programming," *Mathematical Programming*, vol. 106, no. 1, pp. 25–57, 2006.

[14] R. Fourer, D. M. Gay, and B. W. Kernighan, *AMPL: A Modeling Language for Mathematical Programming*, San Francisco, CA, USA: Scientific, 2003.